



Cite this: *RSC Adv.*, 2018, 8, 1940

Synthesis and characterization of Mn-doped CsPb(Cl/Br)₃ perovskite nanocrystals with controllable dual-color emission

Pengchao Wang,  Bohua Dong,* Zhenjie Cui, Rongjie Gao, Ge Su, Wei Wang and Lixin Cao*

Metal-halide perovskite nanocrystals (NCs) are considered to be promising types of optoelectronic and photonic materials. The emission colors of the cesium lead halide perovskite (CsPbX₃, X = Cl, Br, I) NCs depend on the joint influence of the emission peaks of the host and its dopant ions. Herein, we report a phosphine-free strategy to synthesize Mn-doped CsPb(Cl/Br)₃ NCs to tune their optical properties in a wide color gamut. Colloidal Mn-doped CsPb(Cl/Br)₃ NCs were synthesized by injecting Cs-oleate solution into the MnCl₂ and PbBr₂ precursor solution. The as-prepared Mn-doped CsPb(Cl/Br)₃ NCs are highly crystalline and uniform sized nanocubes with two emission peaks, including the host emission around 450 nm and the Mn²⁺ dopant emission around 600 nm, which are sensitive to the MnCl₂-to-PbBr₂ molar feed ratio and the reaction temperature. By varying the MnCl₂-to-PbBr₂ molar feed ratio or the reaction temperature, the relative PL intensities of dual color emission can be manipulated, showing their ability in tunable color output.

Received 13th December 2017

Accepted 3rd January 2018

DOI: 10.1039/c7ra13306e

rsc.li/rsc-advances

1. Introduction

Solution-processed hybrid and inorganic lead halide perovskites have attracted much attention in the past several years due to their excellent emission properties, high photoluminescence quantum yields (PLQY), small exciton binding energy and balanced electron and hole mobility lifetime,^{1–8} which means that these materials have great potential in photophysical applications, including light emitting diodes, lasers and photodetectors.^{9–19} However, the hybrid lead halide perovskites are extremely sensitive to oxygen and moisture,^{20–22} which greatly restricts their applications. Compared with the organic-inorganic perovskite nanocrystals, the all-inorganic cesium lead halide (CsPbX₃, X = Cl, Br, I) nanocrystals are much more stable. In addition, due to the high photoluminescence quantum yields without any additional surface passivation and tunable optical properties throughout the entire visible spectrum, the CsPbX₃ perovskite nanocrystals have great potential in optoelectronic applications.^{23,24}

Up to date, the synthetic protocols for colloidal perovskite NCs are focused on hot-injection,^{25,26} anion-exchange reactions,^{27–31} room-temperature synthesis,³² and ultrasonication.^{33,34} Kovalenko and his coworkers first synthesized the all-inorganic CsPbX₃ perovskite NCs by injecting the prepared Cs-oleate into an octadecene solution containing PbX₂

(X = Cl, Br, I) and ligands (oleic acid and oleylamine) at a temperature of 140–200 °C.²⁵ Under this method, they prepared monodisperse CsPbX₃ nanocrystals with bright photoluminescence (PL) and narrow full width at half maximum (FWHM). Following their pioneering work, great processes have been made and a variety of shapes of CsPbX₃ NCs, such as cubes,^{25,35} nanowires^{26,36–39} and nanoplatelets, are obtained. Furthermore, the PL spectra of the CsPbX₃ NCs can be tuned over nearly the entire visible spectral region by tuning the composition of the perovskite NCs through the anion-exchange reactions.^{27,29}

The introduction of transition metal ions in II–VI and III–V semiconductor NCs provides another method to adjust the optical, electronic and magnetic properties to afford the parent NCs with brand new functions.^{40–42} The most commonly used transition metal ion is Mn²⁺. And the Mn-doped II–VI semiconductors (ZnS, ZnSe, CdS, CdSe) could generate intense doped luminescence of Mn²⁺ ions, which is attribute to energy transfer from excited host semiconductors to Mn²⁺ ions.⁴³ In consideration of the similar ionic radius and same valence state of Mn²⁺ and Pb²⁺ ions, it is possible to synthesis the Mn-doped CsPbX₃ NCs. The recent progress in synthesizing Mn-doped CsPbCl₃ NCs also confirms its feasibility.^{44,45} Despite the successes in the preparation of Mn-doped CsPbCl₃ NCs, detailed research into the synthesis of Mn-doped CsPb(Cl/Br)₃ NCs and tailoring of its optical properties is still rare.

In this paper, we report the phosphine-free colloidal synthesis of Mn-doped CsPb(Cl/Br)₃ NCs to tune their optical properties in a wide color gamut. The synthesis was performed

School of Materials Science and Engineering, Ocean University of China, 238 Songling Road, Qingdao, 266100, P. R. China. E-mail: dongbohua@ouc.edu.cn; caolixin@ouc.edu.cn



by injecting Cs-oleate solution into the PbBr_2 and MnCl_2 precursor solution. The as-prepared Mn-doped $\text{CsPb}(\text{Cl}/\text{Br})_3$ NCs are highly crystalline and uniform sized nanocubes with two emission peaks, including the host emission around 450 nm and the Mn^{2+} dopant emission around 600 nm, which are both sensitive to the MnCl_2 -to- PbBr_2 molar feed ration or the reaction temperature. By changing the MnCl_2 -to- PbBr_2 molar feed ration or the reaction temperature, the relative PL intensities of dual color emission can be well manipulated and shows a wide color gamut, indicating their potential in light emitting devices.

2. Experimental

2.1 Chemicals

Cesium carbonate (Cs_2CO_3 , 99%), lead bromide (PbBr_2 , 99%), manganese chloride (MnCl_2 , $\geq 99\%$), 1-octadecene (ODE, $\geq 90\%$), oleic acid (OA, 90%), oleylamine (OAm, 80–90%) and cyclohexane (CYH, $\geq 99\%$) were purchased from Shanghai Aladdin Industrial Corporation Co., Ltd. Acetone was purchased from Yantai Far Eastern Fine Chemical Co., Ltd. All chemicals were used without any further purification.

2.2 Preparation method

2.2.1 Preparation of Cs-oleate. 0.1625 g of Cs_2CO_3 was mixed with 10 mL of ODE and 1 mL of OA in a 100 mL 3-neck flask. The mixture was degassed and dried under vacuum at 120 °C for an hour to remove the water, and then heated to 150 °C under Ar flow for half an hour until all Cs_2CO_3 reacted with OA.

2.2.2 Synthesis of Mn-doped $\text{CsPb}(\text{Cl}/\text{Br})_3$ NCs. In a typical synthesis, 10 mL of ODE, 1 mL of OAm, 1 mL of OA, 0.0734 g of PbBr_2 and 0.034 g of MnCl_2 were loaded into a 100 mL three-neck

flask and dried under vacuum at 120 °C for 30 min. Then, the temperature was raised to over 200 °C for the complete solubilization of PbBr_2 and MnCl_2 salts. Afterwards, the temperature was lowered to 180 °C and 0.8 mL of Cs-oleate solution (prepared as described above) was injected. The reaction mixture was cooled to room temperature immediately using a water bath. The NCs were isolated by centrifugation at 8000 rpm for 9 min and washed once with acetone. The obtained precipitated NCs were re-dispersed in cyclohexane for further use.

2.3 Characterization

X-ray diffraction (XRD) patterns were measured using a BRUKER D8 ADVANCE X-ray diffractometer with a $\text{CuK}\alpha$ source.

Transmission electron microscope (TEM) images were obtained on a JEOL-JEM 1200 TEM at an accelerating voltage of 100 kV.

Photoluminescence (PL) spectra were collected using an Edinburgh FLS 980 fluorescence spectrophotometer.

High-resolution TEM (HRTEM) images were taken with a FEI Tecnai TEM at an accelerating voltage of 200 kV.

Ultraviolet and visible absorption (UV-vis) spectra were performed by a Shimadzu UV-2550 ultraviolet-visible spectrometer with an integrating sphere.

Inductive coupled plasma (ICP) were taken with a Thermal ICAP 6300 ICP spectrometer to determine the Mn/Pb elemental ratio.

The photoluminescence quantum yields (PLQY) of the nanocrystal samples were obtained by comparing the integrated PL intensities of the nanocrystals and the standard dye (quinine sulfate), with 55.7% PLQY in 0.1 mol L^{-1} H_2SO_4 under 320 nm exciton source. Refractive index of 0.1 mol L^{-1} H_2SO_4 and

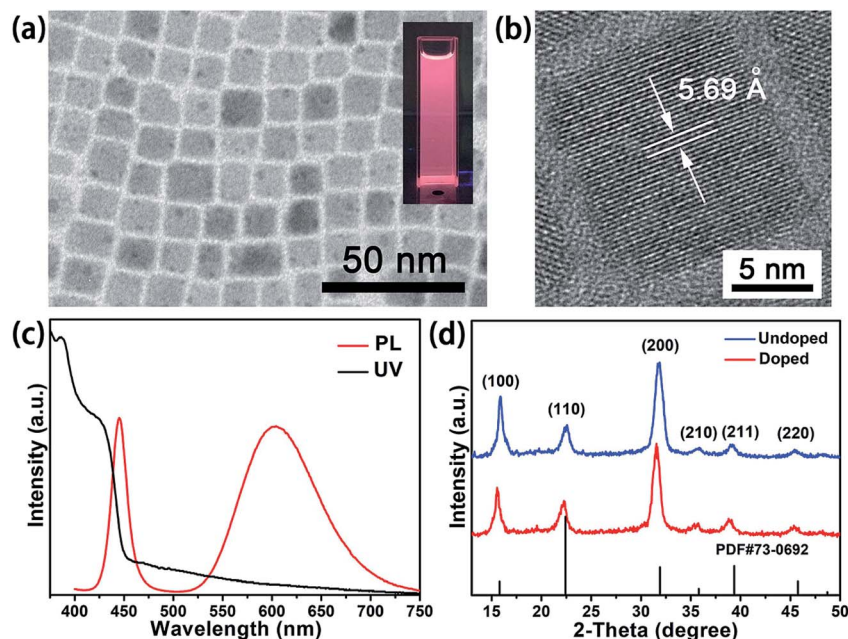


Fig. 1 TEM image (a), HRTEM image (b), PL emission and UV-vis absorption spectra (c) and XRD pattern of Mn-doped $\text{CsPb}(\text{Cl}/\text{Br})_3$ NCs (d). Inset in (a): PL image excited by 365 nm UV light.



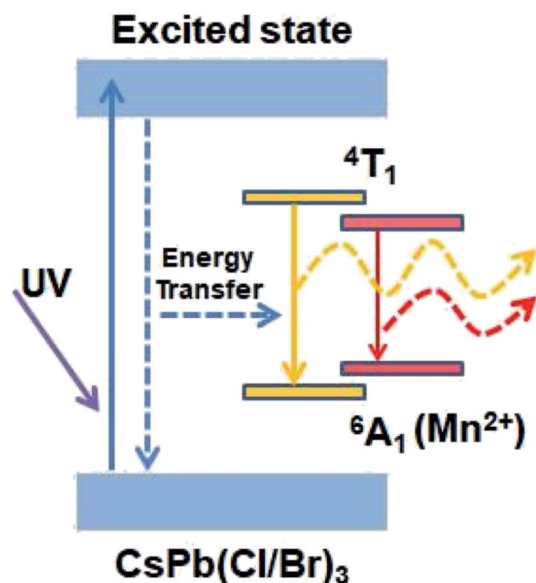


Fig. 2 Energy levels and fluorescent mechanism of Mn-doped CsPb(Cl/Br)₃ NCs.

cyclohexane were 1.344 and 1.427, respectively. According to the following formula, PLQY could be obtained:

$$\Phi_{f1}/\Phi_{f2} = F_1/F_2 \times A_2/A_1(\eta_1/\eta_2)^2$$

where Φ_{f2} is the PLQY of the standard dye, A is the absorption of the solution, F is the integrated emission intensity and η is the average refractive indices of the solution.

3. Results and discussion

The Mn-doped CsPb(Cl/Br)₃ NCs are prepared in colloidal solution by introducing MnCl₂ into PbBr₂ precursors. In a typical synthesis, MnCl₂ and PbBr₂ with the molar feed ratio of 1.35 are mixed in a mixture of OA, OAm and ODE under vacuum at 120 °C to remove the water. Then it is vital important to raise the temperature over 200 °C for the complete solubilization of the metal salts. Afterwards, the temperature is lowered to 180 °C

and Cs-oleate solution is rapidly injected into the precursor solution to get the Mn-doped CsPb(Cl/Br)₃ NCs. The nanostructures of the as-prepared Mn-doped CsPb(Cl/Br)₃ NCs were obtained with TEM. TEM image in Fig. 1a shows that the as-prepared Mn-doped CsPb(Cl/Br)₃ NCs have a cubic morphology with a uniform average size of 11.5 nm. X-ray diffraction (XRD) was used to elucidate the phase structure of the Mn-doped CsPb(Cl/Br)₃ NCs. As shown in Fig. 1d, all of the diffraction peaks of Mn-doped CsPb(Cl/Br)₃ NCs moved slightly to lower angles compared to the undoped cubic CsPbCl₃ nanocrystals (space group *Pm3m*, PDF#73-0692). This could be attributed to the incorporation of Br[−] ions into CsPbCl₃ NCs, which leads to the expansion of the cell, so all the peaks move to lower angles. The XRD also shows that the as-prepared Mn-doped CsPb(Cl/Br)₃ NCs could be ascribed to the same cubic phase with undoped CsPbCl₃ NCs, which means the doping process do not affect the cubic perovskite crystal structure as a result of the rigidity of its cationic framework. High-resolution TEM (HRTEM) image (Fig. 1b) reveals an interplanar spacing of 5.69 Å for its (100) plane set, which is larger than the 5.6 Å of CsPbCl₃. This also confirms the host of the as-prepared Mn-doped NC is CsPb(Cl/Br)₃. The width of the XRD peaks and the HRTEM image reflects the high crystalline nature of the Mn-doped CsPb(Cl/Br)₃ NCs.

The optical properties of the as-synthesized Mn-doped CsPb(Cl/Br)₃ NCs were studied by measuring ultraviolet and visible absorption (UV-vis) spectra and photoluminescence (PL) spectra of the material dispersed in cyclohexane (Fig. 1c). The inset of Fig. 1a shows that the solution of Mn-doped CsPb(Cl/Br)₃ NCs exhibits a deep pink color emission under a 365 nm UV-lamp. The absorption peak of the Mn-doped CsPb(Cl/Br)₃ NCs is around 424 nm. The PL spectra shows distinctive dual color emissions. The narrow band emission centered at 445 nm with FWHM 18 nm is assigned to the CsPb(Cl/Br)₃ host. And, the broad emission centered at 603 nm with FWHM 87.5 nm is assigned to the Mn²⁺ ions doped in the CsPb(Cl/Br)₃ NCs, which can be attribute to a transition between ⁴T₁ and ⁶A₁ energy levels of the Mn²⁺ 3d states. The energy levels and fluorescent mechanism of Mn-doped CsPb(Cl/Br)₃ NCs is shown in Fig. 2. The intense Mn²⁺ luminescence indicates that the doped Mn²⁺ ions

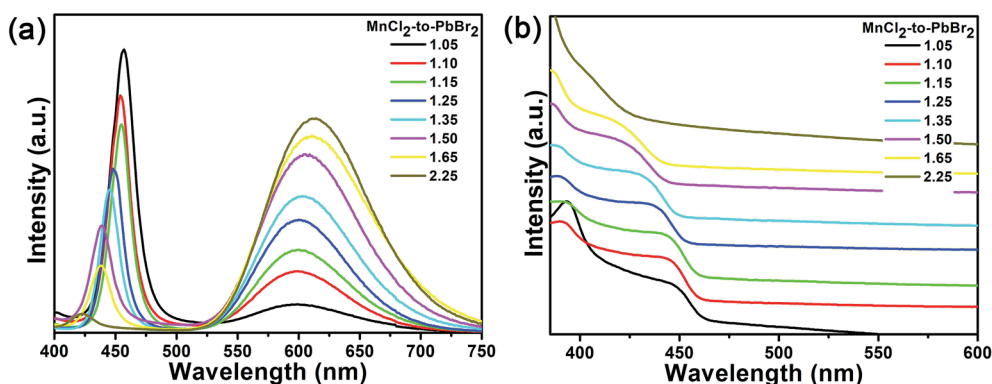


Fig. 3 PL emission spectra (a) and absorption spectra (b) of the Mn-doped CsPb(Cl/Br)₃ NCs prepared with different MnCl₂-to-PbBr₂ molar feed ratio at 180 °C.



Table 1 The PLQYs of the Mn-doped CsPb(Cl/Br)₃ NCs prepared with different MnCl₂-to-PbBr₂ molar feed ratio and reaction temperature

MnCl ₂ -to-PbBr ₂ molar feed ratio	Reaction temperature (°C)	PLQY (%)
1.05	180	14.3
1.10	180	15.6
1.15	180	16.8
1.25	180	22.1
1.35	180	25.7
1.50	180	34.6
1.65	180	38.2
2.25	180	37.1
1.35	160	15.0
1.35	200	33.9

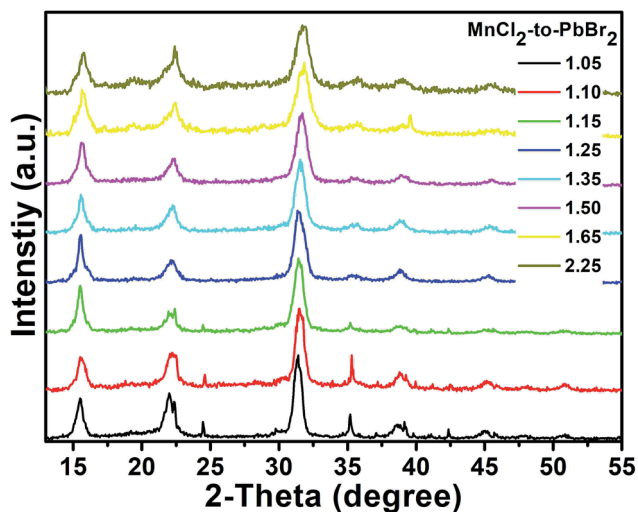


Fig. 4 XRD patterns of the Mn-doped CsPb(Cl/Br)₃ NCs with different MnCl₂-to-PbBr₂ molar feed ratio.

could be served as an efficient acceptor of the energy from the excited CsPb(Cl/Br)₃ host. Although no evidence from microscopy that Mn²⁺ ions is incorporated into the lattice of the nanocrystal, the PL spectrum sufficiently confirms the existence of Mn²⁺ ions in the as-prepared CsPb(Cl/Br)₃ NCs.

The optical properties of the Mn-doped CsPb(Cl/Br)₃ NCs can be tailored by tuning the MnCl₂-to-PbBr₂ molar feed ration. By fixing the reaction temperature at 180 °C, the PL spectrum of the Mn-doped CsPb(Cl/Br)₃ NCs with different MnCl₂-to-PbBr₂ molar feed ratio (from 1.05 to 2.25) is shown in Fig. 3a. As mentioned above, there are two emissions of the Mn-doped CsPb(Cl/Br)₃ NCs, the emission of CsPb(Cl/Br)₃ host and Mn²⁺ ions respectively. By increasing the MnCl₂-to-PbBr₂ molar feed ratio, the narrow PL emission of the CsPb(Cl/Br)₃ host shows a blue shift from 457 to 422 nm, which is attribute to the increase of the Cl-to-Br molar ratio in the CsPb(Cl/Br)₃ host. The change of the Br-to-Cl molar ratio also leads to a slight blue shift of the UV-vis absorption (Fig. 3b). At the same time, the broad emission of the Mn²⁺ ions shows a red shift from 597 nm to 613 nm. This is attributed to the formation of more Mn-to-Mn pairs with the increasing Mn percentage,^{46,47} which decreased the energy gap of ⁴T₁-⁶A₁ (Fig. 2) and resulted the red shifting of Mn²⁺ ions emission. With relatively low MnCl₂-to-PbBr₂ molar feed ratio, the Mn²⁺ substitution ratio in the CsPb(Cl/Br)₃ host is not high. So the CsPb(Cl/Br)₃ host would compete with the energy transfer of Mn²⁺ ions and quench its emission. However, by increasing the MnCl₂-to-PbBr₂ molar feed ratio, the Mn²⁺ substitution ratio in the CsPb(Cl/Br)₃ host increases, which lead to the enhancement of exciton-to-Mn²⁺ energy transfer. The elemental ratio was determined with inductive coupled plasma (ICP). When the MnCl₂-to-PbBr₂ molar feed ratio is increased from 1.05 to 2.25, the Mn²⁺ substitution ratio increases from 1.50 to 2.33%. So, the emission of Mn²⁺ ions is greatly enhanced and the emission of the CsPb(Cl/Br)₃ host gradually faded,

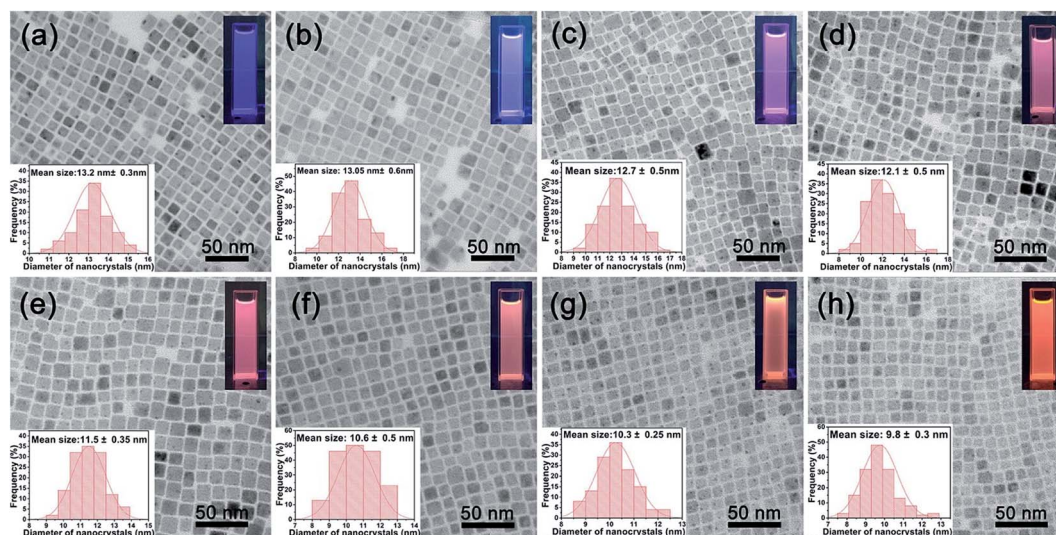


Fig. 5 Transmission electron microscope (TEM) images of the Mn-doped CsPb(Cl/Br)₃ NCs with different MnCl₂-to-PbBr₂ molar feed ratio: (a) 1.05, (b) 1.10, (c) 1.15, (d) 1.25, (e) 1.35, (f) 1.50, (g) 1.65, (h) 2.25. Insets: corresponding particle size distribution and PL images excited by 365 nm UV light.



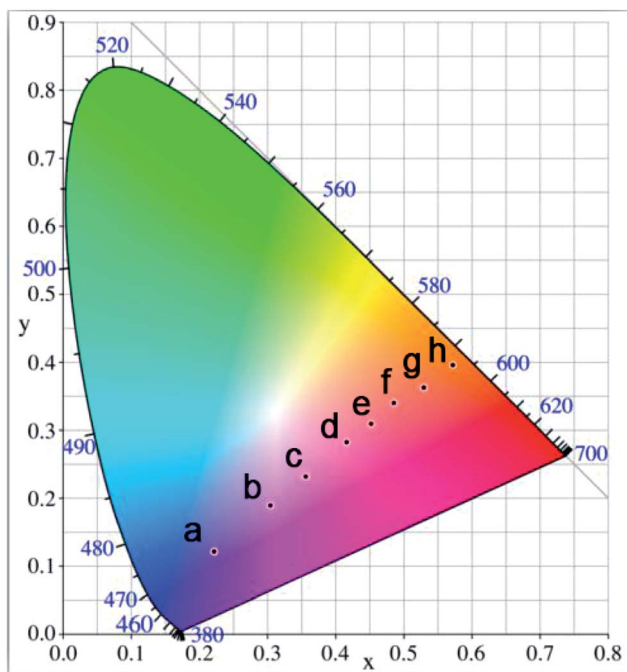


Fig. 6 CIE chromaticity diagram of the Mn-doped $\text{CsPb}(\text{Cl}/\text{Br})_3$ NCs prepared with different MnCl_2 -to- PbBr_2 molar feed ratio: (a) 1.05, (b) 1.10, (c) 1.15, (d) 1.25, (e) 1.35, (f) 1.50, (g) 1.65, (h) 2.25.

which result in the increase of the orange emission. And, with increasing PL intensity of Mn^{2+} ions, the PLQYs of the Mn-doped $\text{CsPb}(\text{Cl}/\text{Br})_3$ NCs prepared with the 1.05 to 1.65 MnCl_2 -

to- PbBr_2 molar feed ratio also increase from 14.3 to 38.2%. The PLQYs of the prepared NCs with 2.25 MnCl_2 -to- PbBr_2 molar feed ratio is slightly lowered to 37.1%, which is much attributed to the decrease of the host PLQY. The PLQYs of the Mn-doped $\text{CsPb}(\text{Cl}/\text{Br})_3$ NCs prepared with different MnCl_2 -to- PbBr_2 molar feed ratio are summarized in Table 1. The above results show that by tuning MnCl_2 -to- PbBr_2 molar feed ratio in the precursor solution, we can precisely control the optical properties of the Mn-doped $\text{CsPb}(\text{Cl}/\text{Br})_3$ NCs.

Fig. 4 shows the XRD patterns of the Mn-doped $\text{CsPb}(\text{Cl}/\text{Br})_3$ NCs with different MnCl_2 -to- PbBr_2 molar feed ratio (from 1.05 to 2.25). All the patterns of the Mn-doped NCs could be ascribed to the same cubic phase, which further proves that the Mn-doped $\text{CsPb}(\text{Cl}/\text{Br})_3$ NCs prepared at different MnCl_2 -to- PbBr_2 molar feed ratio retain their stable structure and possess the same crystalline structure of cubic CsPbCl_3 (PDF#73-0692). We can also observe that all of the diffraction peaks of the XRD patterns shift to higher angles with the increase of the MnCl_2 -to- PbBr_2 molar feed ratio. Because, the combination of Cl^- ions leads to the shrink of the cell and all the peaks move to higher angles. These results are similar with the anion exchange reactions using Pb-based halide precursors or oleylammonium halide precursors in the previous reports.²⁷

The nanostructures of the as-prepared Mn-doped $\text{CsPb}(\text{Cl}/\text{Br})_3$ NCs were obtained with TEM. TEM images in Fig. 5 show that the samples prepared at different MnCl_2 -to- PbBr_2 molar feed ratio exhibit similar cubic morphology and slight size variation. With the increase of the MnCl_2 -to- PbBr_2 molar feed ratio from 1.05 to 2.25, the size of the as-prepared Mn-doped $\text{CsPb}(\text{Cl}/\text{Br})_3$ NCs gradually decreases. The insets of the TEM

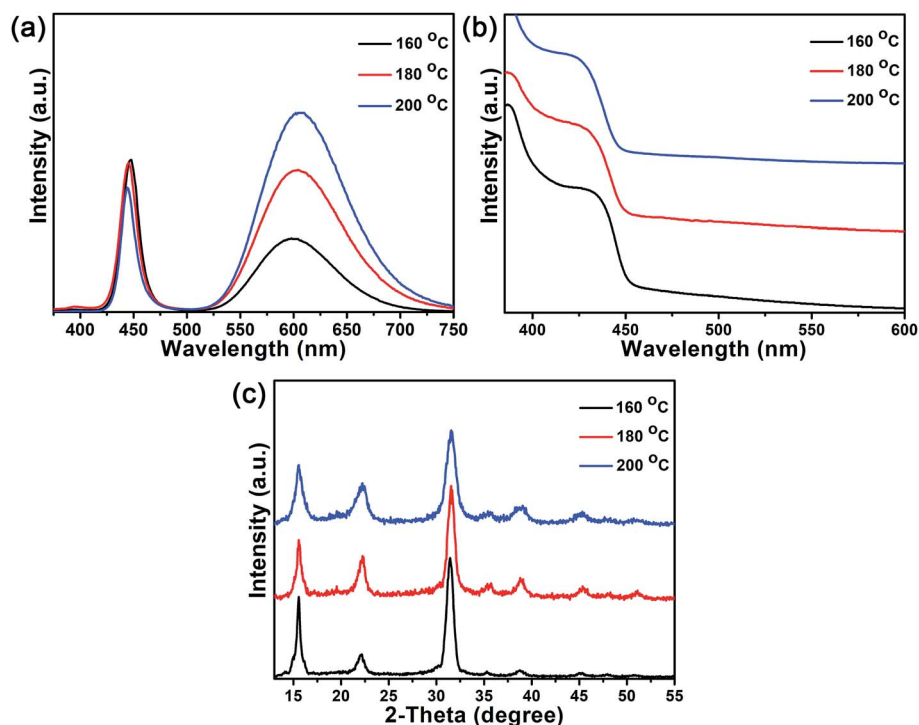


Fig. 7 PL emission spectra (a) absorption spectra (b) and XRD patterns (c) of the Mn-doped $\text{CsPb}(\text{Cl}/\text{Br})_3$ NCs that are prepared at 160, 180 and 200 °C with the MnCl_2 -to- PbBr_2 molar feed ratio of 1.35.



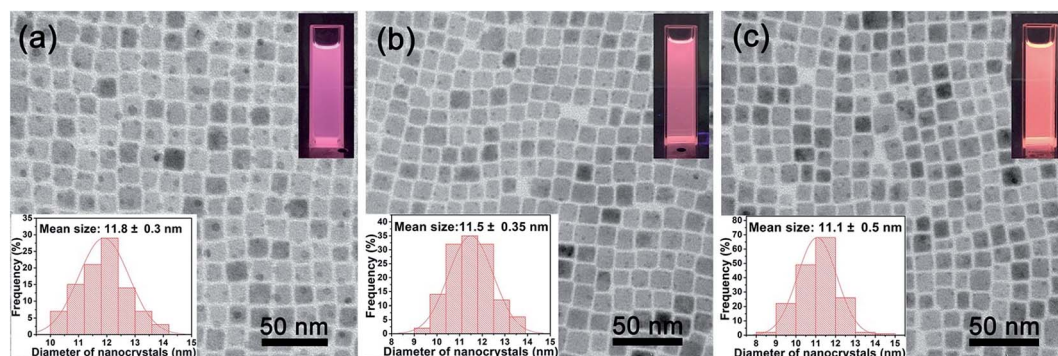


Fig. 8 Transmission electron microscope (TEM) images of the Mn-doped $\text{CsPb}(\text{Cl}/\text{Br})_3$ NCs prepared at different reaction temperature: (a) 160 °C, (b) 180 °C, (c) 200 °C. Insets: corresponding particle size distribution and PL images excited by 365 nm UV light.

images are the corresponding particle size distribution and PL images of the nanocrystal cyclohexane solution excited by 365 nm UV light.

To evaluate the Mn-doped $\text{CsPb}(\text{Cl}/\text{Br})_3$ NCs performance on color luminescent emission with different MnCl_2 -to- PbBr_2 molar feed ratio, CIE (Commission Internationale de l'Eclairage 1931 chromaticity) chromaticity coordinates were concluded and presented in Fig. 6. The graph indicates that the color hue of the Mn-doped $\text{CsPb}(\text{Cl}/\text{Br})_3$ NCs can be tuned precisely, which can be clearly seen from the corresponding PL images of the nanocrystal cyclohexane solution excited by 365 nm UV light (insets of Fig. 5a–h).

Similar to the doping of Mn^{2+} ions into CdSe or ZnSe NCs, the doping of Mn^{2+} ions into $\text{CsPb}(\text{Cl}/\text{Br})_3$ NCs is also a thermodynamics-controlled process.^{48,49} By fixing the MnCl_2 -to- PbBr_2 molar feed ratio at 1.35, the PL spectrum of the Mn-doped $\text{CsPb}(\text{Cl}/\text{Br})_3$ NCs with different reaction temperature is shown in Fig. 7a. The PL spectrum of the Mn-doped $\text{CsPb}(\text{Cl}/\text{Br})_3$ NCs that are prepared at 160, 180 and 200 °C also show two emission peaks, one of the $\text{CsPb}(\text{Cl}/\text{Br})_3$ host at about 445 nm and the other of the Mn^{2+} ions at about 600 nm. With the increase of the reaction temperature (160 to 200 °C), the emission of Mn^{2+} ions shows a red shift from 598 to 605 nm, which is attributed to the formation of more Mn-to-Mn pairs with the increasing Mn percentage. When the reaction temperature is increased from 160 to 200 °C, the Mn^{2+} substitution ratio increases from 1.25 to 2.46%. The increase of the Mn^{2+} substitution ratio lead to the enhancement of exciton-to- Mn^{2+} energy transfer, which strengthened the Mn^{2+} ions emission. So, the PLQYs of the Mn-doped $\text{CsPb}(\text{Cl}/\text{Br})_3$ NCs also increase from 15.0 to 33.9% (Table 1). The doping of Mn^{2+} ions into the $\text{CsPb}(\text{Cl}/\text{Br})_3$ host also causes the absorption spectra blue shift to 426 nm at higher reaction temperature (Fig. 7b), which is similar to that observed in Mn-doped CdSe NCs.⁵⁰ The Mn-doped $\text{CsPb}(\text{Cl}/\text{Br})_3$ NCs prepared at different reaction temperatures retain their stable structure and possess the same crystalline structure of cubic CsPbCl_3 . As the Mn^{2+} substitution ratio do not increase obvious, we can hardly see any shifts of the diffraction peaks during this process.

TEM images in Fig. 8 show that the Mn-doped $\text{CsPb}(\text{Cl}/\text{Br})_3$ NCs prepared at different reaction temperature with the same

molar feed ratio of 1.35 exhibit similar monodispersed cubic morphology and little size variation. This means that the reaction temperature does not influence the basic growth process of the $\text{CsPb}(\text{Cl}/\text{Br})_3$ host. The insets of the TEM images are the corresponding particle size distribution and PL images of the nanocrystal cyclohexane solution excited by 365 nm UV light.

To evaluate the influence of the reaction temperature on color luminescent emission, CIE chromaticity coordinates were concluded and presented in Fig. 9. The corresponding PL images of the nanocrystal cyclohexane solution excited by 365 nm UV light (insets of Fig. 8a–c). Although the reaction temperature has an influence on the optical properties of the Mn-doped $\text{CsPb}(\text{Cl}/\text{Br})_3$ NCs, such an effect is less obvious than the MnCl_2 -to- PbBr_2 molar feed ratio influences.

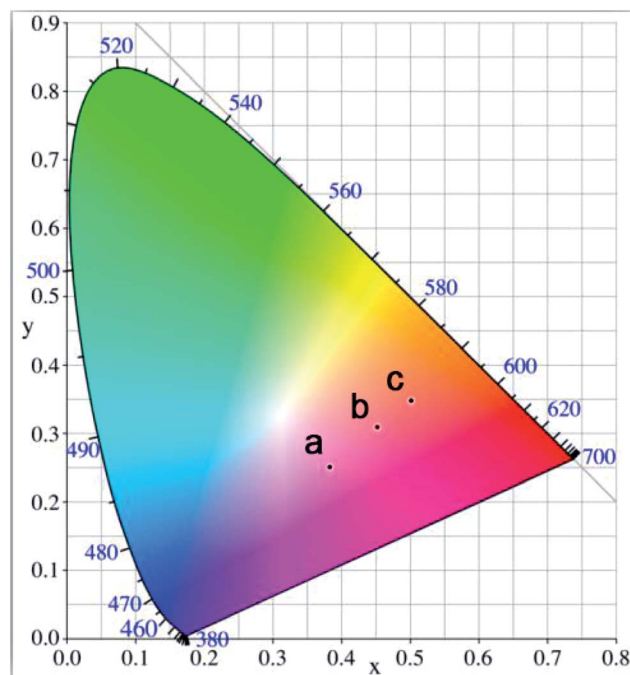


Fig. 9 CIE chromaticity diagram of the Mn-doped $\text{CsPb}(\text{Cl}/\text{Br})_3$ NCs prepared at different reaction temperature: (a) 160 °C, (b) 180 °C, (c) 200 °C.



In conclusion, in this work, we report a phosphine-free strategy to synthesize Mn-doped CsPb(Cl/Br)₃ NCs to tune their optical properties in a wide color gamut. The as-prepared CsPb(Cl/Br)₃ NCs are highly crystalline and uniform sized nanocubes with two emission peaks, including the host emission around 450 nm and the Mn²⁺ dopant emission around 600 nm, which are sensitive to the MnCl₂-to-PbBr₂ molar feed ratio or the reaction temperature. By varying the MnCl₂-to-PbBr₂ molar feed ratio or the reaction temperature, the relative PL intensities of dual color emission can be well manipulated to a wide color gamut, indicating their potential in light emitting devices.

Conflicts of interest

There are no conflicts to declare.

Acknowledgements

We thank National Natural Science Foundation of China (Grants 51372234, and 21301187) for financial support. B. Dong thanks Fundamental Research Funds for the Central Universities (Grant 201564001), project funding by China Postdoctoral Science Foundation (Grant 2015M582132 and 2016T60652), and the Qingdao Science and Technology Plan (Grant 15-9-1-60-jch).

References

- 1 L. Protesescu, S. Yakunin, M. I. Bodnarchuk, F. Krieg, R. Caputo, C. H. Hendon, R. X. Yang, A. Walsh and M. V. Kovalenko, *Nano Lett.*, 2015, **15**, 3692–3696.
- 2 K. Wu, G. Liang, Q. Shang, Y. Ren, D. Kong and T. Lian, *J. Am. Chem. Soc.*, 2015, **137**, 12792–12795.
- 3 G. Rainò, G. Nedelcu, L. Protesescu, M. I. Bodnarchuk, M. V. Kovalenko, R. F. Mahrt and T. Stöferle, *ACS Nano*, 2016, **10**, 2485–2490.
- 4 M. Kulbak, D. Cahen and G. Hodes, *J. Phys. Chem. Lett.*, 2015, **6**, 2452–2456.
- 5 M. M. Lee, J. Teuscher, T. Miyasaka, T. N. Murakami and H. J. Snaith, *Science*, 2012, **338**, 643–647.
- 6 W. S. Yang, J. H. Noh, N. J. Jeon, Y. C. Kim, S. Ryu, J. Seo and S. I. Seok, *Science*, 2015, **348**, 1234–1237.
- 7 N. J. Jeon, J. H. Noh, W. S. Yang, Y. C. Kim, S. Ryu, J. Seo and S. I. Seok, *Nature*, 2015, **517**, 476–480.
- 8 M. Grätzel, *Nat. Mater.*, 2014, **13**, 838–842.
- 9 S. D. Stranks and H. J. Snaith, *Nat. Nanotechnol.*, 2015, **10**, 391–402.
- 10 H. Zhu, Y. Fu, F. Meng, X. Wu, Z. Gong, Q. Ding, M. V. Gustafsson, M. T. Trinh, S. Jin and X. Zhu, *Nat. Mater.*, 2015, **14**, 636–642.
- 11 P. Ramasamy, D. H. Lim, B. Kim, S. H. Lee, M. S. Lee and J. S. Lee, *Chem. Commun.*, 2016, **52**, 2067–2070.
- 12 Y. Xu, Q. Chen, C. Zhang, R. Wang, H. Wu, X. Zhang, G. Xing, W. W. Yu, X. Wang, Y. Zhang and M. Xiao, *J. Am. Chem. Soc.*, 2016, **138**, 3761–3768.
- 13 S. Yakunin, L. Protesescu, F. Krieg, M. I. Bodnarchuk, G. Nedelcu, M. Humer, G. De Luca, M. Fiebig, W. Heiss and M. V. Kovalenko, *Nat. Commun.*, 2015, **6**, 8056.
- 14 N. Yantara, S. Bhaumik, F. Yan, D. Sabba, H. A. Dewi, N. Mathews, P. P. Boix, H. V. Demir and S. Mhaisalkar, *J. Phys. Chem. Lett.*, 2015, **6**, 4360–4364.
- 15 Q. Zhou, Z. Bai, W. G. Lu, Y. Wang, B. Zou and H. Zhong, *Adv. Mater.*, 2016, **28**, 9163–9168.
- 16 G. Li, Z. K. Tan, D. Di, M. L. Lai, L. Jiang, J. H. Lim, R. H. Friend and N. C. Greenham, *Nano Lett.*, 2015, **15**, 2640–2644.
- 17 J. Liang, Y. Zhang, X. Guo, Z. Gan, J. Lin, Y. Fan and X. Liu, *RSC Adv.*, 2016, **6**, 71070–71075.
- 18 X. J. Ma, Z. Q. Wang, Z. Y. Xiong, Y. Zhang, F. X. Yu, P. Chen, Z. H. Xiong and C. H. Gao, *RSC Adv.*, 2017, **7**, 50571–50577.
- 19 X. Du, G. Wu, J. Cheng, H. Dang, K. Ma, Y. W. Zhang, P. F. Tan and S. Chen, *RSC Adv.*, 2017, **7**, 10391–10396.
- 20 M. B. Teunis, K. N. Lawrence, P. Dutta, A. P. Siegel and R. Sardar, *Nanoscale*, 2016, **8**, 17433–17439.
- 21 S. Gonzalez-Carrero, R. E. Galian and J. Pérez-Prieto, *J. Mater. Chem. A*, 2015, **3**, 9187–9193.
- 22 H. Huang, A. S. Sussha, S. V. Kershaw, T. F. Hung and A. L. Rogach, *Adv. Sci.*, 2015, **2**, 1500194.
- 23 J. Song, J. Li, X. Li, L. Xu, Y. Dong and H. Zeng, *Adv. Mater.*, 2015, **27**, 7162–7167.
- 24 L. Polavarapu, B. Nickel, J. Feldmann and A. S. Urban, *Adv. Energy Mater.*, 2017, **7**, 1700267.
- 25 L. Protesescu, S. Yakunin, M. I. Bodnarchuk, F. Krieg, R. Caputo, C. H. Hendon, R. X. Yang, A. Walsh and M. V. Kovalenko, *Nano Lett.*, 2015, **15**, 3692–3696.
- 26 D. Zhang, S. W. Eaton, Y. Yu, L. Dou and P. Yang, *J. Am. Chem. Soc.*, 2015, **137**, 9230–9233.
- 27 Q. A. Akkerman, V. D'Innocenzo, S. Accornero, A. Scarpellini, A. Petrozza, M. Prato and L. Manna, *J. Am. Chem. Soc.*, 2015, **137**, 10276–10281.
- 28 C. Guhrenz, A. Benad, C. Ziegler, D. Haubold, N. Gaponik and A. Eychmüller, *Chem. Mater.*, 2016, **28**, 9033–9040.
- 29 G. Nedelcu, L. Protesescu, S. Yakunin, M. I. Bodnarchuk, M. J. Grotevent and M. V. Kovalenko, *Nano Lett.*, 2015, **15**, 5635–5640.
- 30 D. Zhang, Y. Yang, Y. Bekenstein, Y. Yu, N. A. Gibson, A. B. Wong, S. W. Eaton, N. Kornienko, Q. Kong, M. Lai, A. P. Alivisatos, S. R. Leone and P. Yang, *J. Am. Chem. Soc.*, 2016, **138**, 7236–7239.
- 31 P. Wang, B. Dong, Z. Cui, R. Gao, G. Su, W. Wang and L. Cao, *Inorg. Chim. Acta*, 2017, **467**, 251–255.
- 32 X. Li, Y. Wu, S. Zhang, B. Cai, Y. Gu, J. Song and H. Zeng, *Adv. Funct. Mater.*, 2016, **26**, 2435–2445.
- 33 Y. Tong, E. Bladt, M. F. Aygüler, A. Manzi, K. Z. Milowska, V. A. Hintermayr, P. Docampo, S. Bals, A. S. Urban and L. Polavarapu, *Angew. Chem., Int. Ed.*, 2016, **55**, 13887–13892.
- 34 V. A. Hintermayr, A. F. Richter, F. Ehrat, M. Doblinger, W. Vanderlinden, J. A. Sichert, Y. Tong, L. Polavarapu, J. Feldmann and A. S. Urban, *Adv. Mater.*, 2016, **28**, 9478–9485.
- 35 I. Lignos, S. Stavrakis, G. Nedelcu, L. Protesescu, A. J. deMello and M. V. Kovalenko, *Nano Lett.*, 2016, **16**, 1869–1877.
- 36 M. C. Weidman, M. Seitz, S. D. Stranks and W. A. Tisdale, *ACS Nano*, 2016, **10**, 7830–7839.



- 37 Q. A. Akkerman, S. G. Motti, A. R. Srimath Kandada, E. Mosconi, V. D'Innocenzo, G. Bertoni, S. Marras, B. A. Kamino, L. Miranda, F. De Angelis, A. Petrozza, M. Prato and L. Manna, *J. Am. Chem. Soc.*, 2016, **138**, 1010–1016.
- 38 J. A. Sichert, Y. Tong, N. Mutz, M. Vollmer, S. Fischer, K. Z. Milowska, R. Garcia Cortadella, B. Nickel, C. Cardenas-Daw, J. K. Stolarczyk, A. S. Urban and J. Feldmann, *Nano Lett.*, 2015, **15**, 6521–6527.
- 39 Y. Tong, B. J. Bohn, E. Bladt, K. Wang and P. Muller-Buschbaum, *Angew. Chem., Int. Ed.*, 2017, **56**, 13887–13892.
- 40 D. A. Schwartz, N. S. Norberg, Q. P. Nguyen, J. M. Parker and D. R. Gamelin, *J. Am. Chem. Soc.*, 2003, **125**, 13205–13218.
- 41 K. E. Knowles, H. D. Nelson, T. B. Kilburn and D. R. Gamelin, *J. Am. Chem. Soc.*, 2015, **137**, 13138–13147.
- 42 F. Meinardi, A. Colombo, K. A. Velizhanin, R. Simonutti, M. Lorenzon, L. Beverina, R. Viswanatha, V. I. Klimov and S. Brovelli, *Nat. Photonics*, 2014, **8**, 392–399.
- 43 R. Beaulac, P. I. Archer, S. T. Ochsenbein and D. R. Gamelin, *Adv. Funct. Mater.*, 2008, **18**, 3873–3891.
- 44 H. Liu, Z. Wu, J. Shao, D. Yao, H. Gao and Y. Liu, *ACS Nano*, 2017, **11**, 2239–2247.
- 45 D. Parobek, B. J. Roman, Y. Dong, H. Jin, E. Lee, M. Sheldon and D. H. Son, *Nano Lett.*, 2016, **16**, 7376–7380.
- 46 H. Y. Chen, S. Maiti and D. H. Son, *ACS Nano*, 2012, **6**, 583–591.
- 47 V. K. Sharma, S. Gokyar, Y. Kelestemur, T. Erdem, E. Unal and H. V. Demir, *Small*, 2014, **10**, 4961–4966.
- 48 D. Magana, S. C. Perera, A. G. Harter, N. S. Dalal and G. F. Strouse, *J. Am. Chem. Soc.*, 2006, **128**, 2931–2939.
- 49 N. Y. D. J. Norris, F. T. Charnock and T. A. Kennedy, *Nano Lett.*, 2001, **1**, 3–7.
- 50 V. A. Vlaskin, C. J. Barrows, C. S. Erickson and D. R. Gamelin, *J. Am. Chem. Soc.*, 2013, **135**, 14380–14389.

